

# A Receiver with in-band $IIP_3 > 20\text{dBm}$ , exploiting Cancelling of OpAmp Finite-Gain-induced Distortion via Negative Conductance

Dlovan H. Mahrof, Eric A.M. Klumperink, Mark S. Oude Alink, and Bram Nauta

University of Twente, IC Design group, Enschede, The Netherlands

**Abstract** — Highly linear CMOS radio receivers increasingly exploit linear RF V-I conversion and passive down-mixing, followed by an OpAmp based Transimpedance Amplifier at baseband. Due to the finite OpAmp gain in wideband receivers operating with large signals, virtual ground is imperfect, inducing distortion currents. We propose to apply a negative conductance to cancel this distortion. In an RF receiver, this increases In-Band  $IIP_3$  from 9dBm to  $>20\text{dBm}$ , at the cost of 1.5dB extra NF and  $<10\%$  power penalty. In 1MHz bandwidth, a Spurious-Free Dynamic Range of 85dB is achieved at  $<27\text{mA}$  up to 2GHz for 1.2V supply voltage.

**Index Terms** — Receiver linearity, in-band and out-band  $IIP_3$ , mixer-first receiver architecture, operational amplifier.

## I. INTRODUCTION

Linearity requirements on radio receivers are increasingly challenging. Fig. 1 plots an example of an  $IIP_3$  requirement calculated for E-UTRA for a wideband base station receiver [1]. Apart from the 100MHz bandwidth, note the sudden step in  $IIP_3$  requirements at the band-edge. Also note that less coverage area (home versus wide area), corresponds to higher in-band  $IIP_3$  but a smaller step to out-of-band  $IIP_3$ . As cost effective filtering is ineffective to reduce the  $IIP_3$  requirement (a reasonable transition band lacks), we aim for new circuit techniques that simultaneously increase in- and out-of-band linearity.

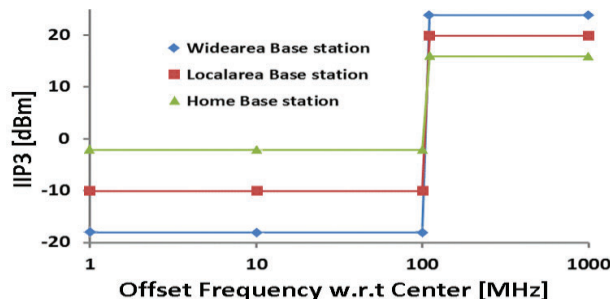


Figure 1: Example  $IIP_3$  requirement for E-UTRA [1]

High-linearity receivers are also very much wanted for opportunistic dynamic spectrum access via a cognitive radio. Assuming a channelized system, strong interferers may be present in directly adjacent channels, again making RF filtering ineffective. Such strong interferers easily clip amplifiers, while higher required bandwidths

limit the amount of available loopgain for negative feedback.

When pushing linearity, avoiding voltage gain at RF is instrumental [2,3,4,5,6]. Exploiting RF V-I conversion followed by passive down-mixing and then simultaneous I-V conversion and filtering at IF/baseband with OpAmps, an out-of-band  $IIP_3$  around  $+15\text{dBm}$  has been shown [2,3]. Passive mixer-first architectures can even achieve up to  $+25\text{dBm}$  out-of-band  $IIP_3$  [6]. However their in-band  $IIP_3$  is much worse. The best in-band  $IIP_3$  achieved were  $+3.5\text{dBm}$  for [2] and  $+11\text{dBm}$  for [5]. Analysis shows that finite OpAmp gain is a bottleneck, as non-zero virtual ground (VGND) node voltages can result in distortion currents. In [2] the in-band linearity was limited to  $+3.5\text{dBm}$  by the OpAmp, while the RF V-I converter achieved  $+18\text{dBm}$   $IIP_3$  [2]. We propose here to use a negative conductance technique to cancel distortion currents. In this way, the design of the OpAmp is relaxed and its performance no longer needs to be a bottleneck. Using a negative conductance has been proposed in [7] to realize TIA flicker noise shaping, but linearity benefits were not reported. Such benefits are discussed next.

## II. PROPOSED LINEARIZATION TECHNIQUE

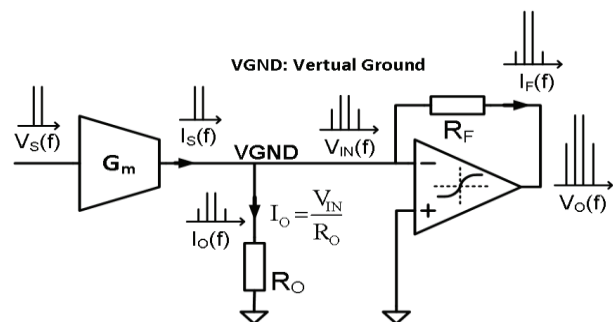


Figure 2: Baseband model for distortion due to the output stage

For analysis, assume the RF V-I conversion and mixing are perfectly linear but do have finite output resistance  $R_O$ . Fig. 2 shows an equivalent baseband model (omitting the downconversion for simplicity). Now, if the OpAmp handles large signals, its output stage will produce  $IM_3$  products (see Fig.2). Due to finite OpAmp gain, the “virtual ground” node VGND also contains  $IM_3$  tones. This voltage produces a (nonlinear!) current in  $R_O$ .

Consequently, even if  $I_S$  is free of  $IM_3$  products, a nonlinear current  $I_O$  is added and the sum of these currents,  $I_F$ , produces a non-linear voltage across  $R_F$ .

By introducing a negative conductance ( $|-G_O|=1/R_O$ ) at VGND, the nonlinear current  $I_O$  flows via ground instead of through  $R_F$  (see Fig.3). Now current  $I_F$  is equal to  $I_S$  and thus free of distortion. Still, the OpAmp output voltage contains some  $IM_3$ , equal to that on the VGND node. By slight overcompensation ( $|-G_O|=1/R_O+1/R_F$ ) this  $IM_3$  contribution can also be cancelled, due to the loading effect of  $R_F$  on VGND. Note that the nonlinearity of the negative conductance is not critical, as swing on VGND is low. The main disadvantage is the added noise of  $-G_O$ .

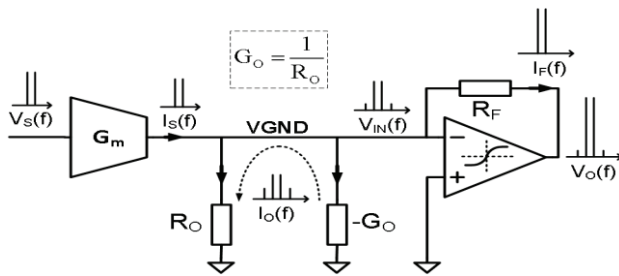


Figure 3: Baseband model with negative conductance solution

### III RECEIVER DESIGN

To demonstrate the linearity potential of this technique we replace the active V-I conversion by a more linear fully passive mixer with resistors in series [3], as shown in Fig.4. We can still model the RF part as a resistors to ground and an equivalent  $G_m = 1/(R_{RF}+R_{ON-MIXER}+R_{VGND})$ , which is chosen 20 mS to realize RF impedance matching. The equivalent output impedance of the mixer at baseband now is  $R_O=2(R_{BalUn}+R_{RF}+R_{ON-MIXER})$ , where the factor 2 is due to the quadrature mixer with 25% duty cycle, connecting each I and Q baseband part to RF two times per LO cycle. Fig.4 shows the front-end IC schematic. The 50Ω matching is implemented as a combination of a series resistances  $R_{RF} \approx 12\Omega$ , the up-converted impedances of the passive mixer switches  $R_{ON-MIXER} \approx 28\Omega$  plus the VGND impedance  $R_{VGND} \approx 7\Omega$ . The passive mixer consists of simple NMOS switches with 25% duty cycle.  $C_O = 8\text{ pF}$  effectively shorts the LO leakage and high IF frequency components. The TIA consists of a class-A input stage and a class-AB output stage, to maximize output swing [2]. Common mode feedback ensures biasing at  $VDD/2$ . The feedback impedance is  $R_F = 1.5\text{ k}\Omega$  and  $C_F = 8\text{ pF}$ , to obtain 26dB voltage gain and a -3dB-bandwidth of 12 MHz. The differential topology allows for a simple differential implementation of the negative conductance (right part of Fig.4) and high  $IIP_2$ . To show what happens

for different negative conductance values,  $-G_O$  is implemented as a parallel array, digitally controllable via multiplier  $M$ , with 0.2mS transconductance steps. Thus  $M=28$  renders  $G_O=5.6\text{mS}$  to compensate  $R_O=180\Omega$  ( $R_O = 2(R_{BalUn}+R_{RF}+R_{ON-MIXER}) = 2(50+12+28) = 180\Omega$ ). In a practical system it will be required to detect distortion and calibrate the  $M$ -value. This may be done during IC test or in operation when on-chip spectrum analysis is available (also wanted for spectrum sensing).

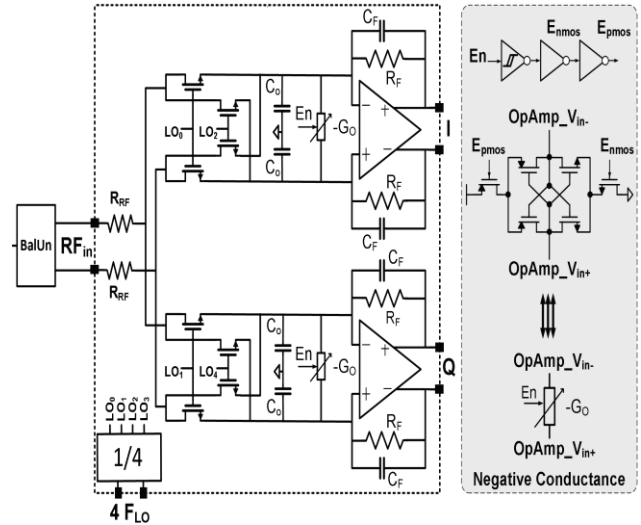


Figure 4: Receiver with distortion compensation by  $-G_O$

### IV MEASUREMENT RESULTS AND COMPARISON

Fig.5 shows a photo of the implemented 65nm IC. The active area is  $< 0.2\text{ mm}^2$  including the clock circuit. Thick metal was used for  $R_{RF}$  for high linearity and low spread.

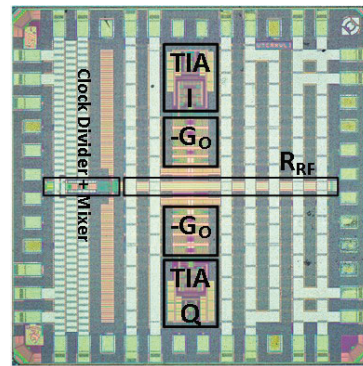


Figure 5: Die Photograph (65nm CMOS, 1.45mm x 1.45mm)

The front-end achieves 26 dB gain (BalUn losses are de-embedded) at 1 GHz LO, over 24MHz bandwidth BW, 12MHz on either side of LO. The compression point (CP) is around -13 dBm (hardly affected by  $M$ ).

To demonstrate distortion cancelling, Fig.6 (top) shows the measured in-band IIP<sub>3</sub> at 150kHz tone spacing vs. M. IIP<sub>3</sub> clearly improves from around +9 dBm to +21 dBm! The negative conductance was pushed to instability. This occurs at M=45, safely away from the optimum point. The optimum IIP<sub>3</sub> of +21 dBm is located at M= 32, while calculation predicts M=28. This difference of 4 is the previously mentioned loading effect of R<sub>F</sub> on the OpAmp virtual ground ( $(1/R_F)/0.2\text{mS}=(1/1500)/0.2\text{mS}=3.33$ ). The negative conductance begins to inject a net current into the feedback resistance R<sub>F</sub> at M > 28 (i.e. after cancelling R<sub>O</sub>). This is verified by simulations.

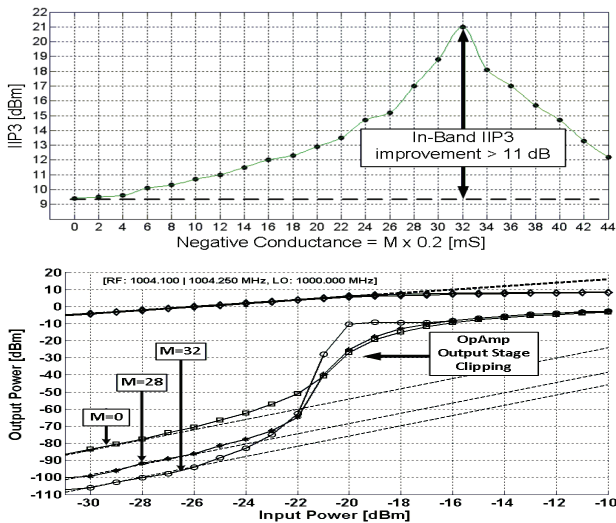


Figure 6: Measured in-band IIP<sub>3</sub> vs. M (top) and IM<sub>3</sub> versus input power for 3 settings (bottom), with LO=1GHz

Fig.6 (bottom) shows the IM<sub>3</sub> curves versus power for three cases: M=0 (off), M=28 (cancelling of I<sub>O</sub>) and M=32 (overall optimum IIP<sub>3</sub>). Up to -22dBm, IM<sub>3</sub> improves. The rise of distortion for high input powers > -25 dBm is due to direct clipping of the OpAmp output stage to its 1.2 V supply. This technique also improves IIP<sub>2</sub> by more than 10 dB as shown in table I.

Table I: IIP<sub>2</sub> and IIP<sub>3</sub> improvement

| M  | IIP <sub>2</sub> [dBm] | IIP <sub>3</sub> [dBm] |
|----|------------------------|------------------------|
| 0  | 51                     | 9.4                    |
| 28 | 58.4                   | 17                     |
| 32 | 61.2                   | 21                     |

Fig.7 provides IIP<sub>3</sub> curves versus the frequency offset Δf, with fixed 3.95MHz in-band IM<sub>3</sub> position. The negative conductance clearly increases the IIP<sub>3</sub> both in and out of band (all-Band) with worst case IIP<sub>3</sub> > +10 dBm. Out-of-band IIP<sub>3</sub> at Δf > 450 MHz is +18 dBm. Up to 10MHz, in-band IIP<sub>3</sub> is >+20dBm, about 10 dB benefit. The IIP<sub>3</sub>

reduction between 12MHz and 135MHz is due to the reduction in OTA gain, whereas IIP<sub>3</sub> increases again due to the low pass filtering of C<sub>F</sub>, R<sub>F</sub> and C<sub>O</sub>.

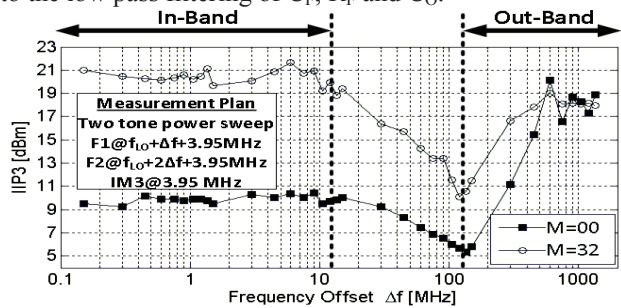


Figure 7: 2-tone IIP<sub>3</sub> measured at IM<sub>3</sub>=3.95MHz versus tone-spacing Δf, with LO=1GHz

Due to the virtual ground, S<sub>11</sub> is hardly affected by the negative conductance and Fig.8 (top) shows that S<sub>11</sub> < -25 dB. Noise is more worrisome, but a bit of degradation can be acceptable, provided that the overall SFDR improves (i.e. IIP<sub>3</sub> in dBm should improve more than NF in dB degrades). Fig.8 (bottom) shows that NF increases from 6.2 dB at M=0 to 7.5 dB at M=32.

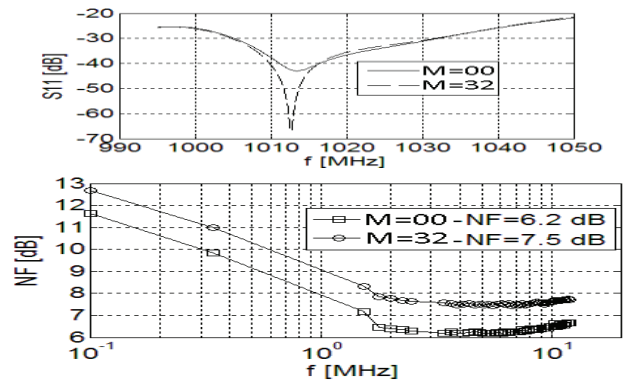


Figure 8: Measured S<sub>11</sub> vs. f<sub>RF</sub> (top) and Noise Figure vs. f<sub>IF</sub> (bottom), with LO=1GHz

The current consumption without the negative conductance at 1 GHz LO is 18 mA (including 8mA of clock circuitry (i.e. on-chip drivers and divider)), and 1.6 mA more for M=32. The clock divider frequency range (i.e. also the receiving RF frequency) is 0.2-2.6 GHz and consumes 2.8-19 mA. The maximum Gate-Source voltage of the mixer switches is equal to 1.2 V supply. The LO leakage to the RF port is less than -75 dBm. The technique used in this paper is robust over spread as the negative conductance is a part of the feedback system. The optimum IIP<sub>3</sub> has been measured for 5 samples. The optimum in-band IIP<sub>3</sub> varies ±1 dB around +21 dBm and the corresponding M varies ±2 around M=32.

Table II: Comparison with other designs

|  | This work                                  | Ru [2]                          | Murphy [3]                 | Youssef [4]                      | Soer [5]                 | Andrews [6]              | units           |
|--|--|---------------------------------|----------------------------|----------------------------------|--------------------------|--------------------------|-----------------|
| Linearization Technique                        | Negative $G_o$                             | Partial cancel Noise/Distortion | Cancel Noise               | Freq. Translated Active feedback | Feedback + N-path filter | Feedback + N-path filter |                 |
| Matching                                       | Switch-R                                   | Common-gate                     | Switch-R                   | R                                | -                        | via TIA                  |                 |
| Mixer type                                     | Switch-R                                   | Switch-I                        | Switch-R&I                 | Gm + Switched-I                  | Switch-RC                | Switch-RC                |                 |
| Baseband-stage                                 | TIA + RC                                   | TIA+RC                          | TIA + RC                   | Inverter-RC                      | Voltage Amp              | TIA+RC                   |                 |
| CMOS Techn.                                    | 65nm                                       | 65nm                            | 40nm                       | 65nm                             | 65nm                     | 65nm                     |                 |
| Active Area                                    | < 0.2                                      | < 1                             | 1.2                        | < 0.06                           | < 0.13                   | 0.75                     | mm <sup>2</sup> |
| RF Frequency                                   | 0.2-2.6                                    | 0.4-0.9                         | 0.08-2.7                   | 1.0-2.5                          | 0.2-2.0                  | 0.1-2.4                  | GHz             |
| Gain   | 26.5                                       | 34                              | 70                         | 30                               | 19                       | 40-70                    | dB              |
| In-band BW <sup>[1]</sup>                      | 24   | 24                              | 4                          | 5                                | 50                       | 1.6                      | MHz             |
| NF   | 7.5  | 4                               | 2                          | 7.25-8.9                         | 6.5                      | 4                        | dB              |
| In-band IIP <sub>3</sub>                       | > +20                                      | +3.5                            | -22                        | -20                              | +11                      | -67                      | dBm             |
| SFDR @ 1MHz bandwidth                          | <b>85</b>                                  | 75                              | 60                         | 57                               | 79                       | 29                       | dB              |
| Wide-Band IIP <sub>3</sub> @ 2-tone $\Delta f$ | $\geq +18$ @ >450<br>>+10 @ All $\Delta f$ | +18<br>@ $\Delta f > 800$       | +13.5<br>@ $\Delta f > 40$ | > +12<br>@ $\Delta f > 60$       | Not measured             | +25<br>@ $\Delta f > 50$ | dBm<br>@ MHz    |
| Supply Voltage                                 | 1.2  | 1.2                             | 1.3                        | 1.2                              | 1.2                      | 1.2 / 2.5                | V               |
| Power Consumption                              | 13.9                                       | 39.6                            | 15.6                       | 62                               | 60                       | < 70 <sup>[2]</sup>      | mW              |

[1] In-band BW is twice the zero-IF bandwidth around the LO frequency

[2] Includes the clock circuitry

Table II benchmarks this work to other state-of-the-art receivers with high linearity and/or SFDR. Our front-end is more linear than [2,4] where active RF blocks are present. Even compared to the mixer-first designs [5,6] we achieve better in-band IIP<sub>3</sub> while our SFDR in 1MHz of 85dB is the highest reported.

## V. CONCLUSION

Due to the strong relationship between linearity and voltage swing, it is challenging to improve linearity in advanced CMOS technologies with lower supply voltages. Architectures with RF VI conversion followed by a passive mixers and TIA (OpAmp with baseband RC filter) perform relatively well. However, for increasing channel bandwidths, the amount of loopgain available for negative feedback is limited. Still high linearity is wanted, not only out-of-band but also in-band, as filtering is often ineffective for close-in interferers (very narrow filter transition band like base stations). This paper proposes to exploit a negative conductance at the virtual ground node in order to clean it from any distortion products induced by the OpAmp output stage. Although, this technique results in slightly degraded noise figure (1.5dB) the in-band IIP<sub>3</sub> (and IIP<sub>2</sub>) is improved by much more (>10dB), resulting the highest reported in-band SFDR=85dB in 1MHz bandwidth in CMOS.

## ACKNOWLEDGEMENT

This research is supported by the Dutch Technology Foundation STW (i.e. the applied science division of the NWO), and the Ministry of Economic Affairs Technology

Program). We thank STMicroelectronics for silicon donation and CMP, Harish K. Subramanian, G. Wienk and H. de Vries for their assistance.

## REFERENCES

- [1] 3GPP TS 36.104: "Evolved Universal Terrestrial Radio Access (E-UTRA); Base Station (BS) radio transmission and reception", available *online*, [www.3gpp.org](http://www.3gpp.org).
- [2] Z. Ru, E.A.M. Klumperink, B. Nauta, "A Software-Defined Radio Receiver Architecture Robust to Out-of-Band Interference," *ISSCC Dig. Tech. Papers*, pp. 230-231, Feb. 2009.
- [3] David Murphy, Amr Hafez, Ahmad Mirzaei, Mohyee Mikhemar, Hooman Darabi, Mau-Chung Frank Chang, Asad Abidi, "A Blocker-Tolerant Wideband Noise-Cancelling Receiver with a 2dB Noise Figure," *ISSCC Dig. Tech. Papers*, pp. 74-76, Feb. 2012.
- [4] S.S.T. Youssef, R.A.R. van der Zee, B. Nauta, "Active Feedback Receiver with Integrated Tunable RF Channel Selectivity, Distortion Cancelling, 48dB Stop-Band Rejection and > +12dBm Wideband IIP<sub>3</sub>, Occupying < 0.06mm<sup>2</sup> in 65nm CMOS," *ISSCC Dig. Tech. Papers*, pp. 166-168, Feb. 2012.
- [5] M.C.M. Soer, E.A.M. Klumperink, Z. Ru, F.E. van Vliet, B. Nauta, "A 0.2-to-2.0GHz 65nm CMOS Receiver Without LNA Achieving >11dBm IIP<sub>3</sub> and <6.5dB NF," *ISSCC Dig. Tech. Papers*, pp. 222-223, Feb. 2009.
- [6] C. Andrews, A.C. Molnar, "A Passive Mixer-First Receiver With Digitally Controlled and Widely Tunable RF Interface," *IEEE J. Solid-State Circ.*, vol. 45, no. 12, pp. 2696-2708, Dec. 2010.
- [7] J. Deguchi et al, "A Fully Integrated 2x1 Dual-Band Direct-Conversion Mobile WiMAX Transceiver With Dual-Mode Fractional Divider and Noise-Shaping Transimpedance Amplifier in 65 nm CMOS," *IEEE J. Solid-State Circ.*, vol. 45, no. 12, pp. 2774 - 2784, Dec. 2010.